

© An Evaluation of NOAA Modeled and In Situ Soil Moisture Values and Variability across the Continental United States

PETER J. MARINESCU^{a,b}, DANIEL ABDI^c, KYLE HILBURN^b, ISIDORA JANKOV^d, AND LIAO-FAN LIN^{b,d}

^a Colorado State University, Fort Collins, Colorado

^b Cooperative Institute for Research in the Atmosphere/Colorado State University, Fort Collins, Colorado

^c Cooperative Institute for Research in Environmental Sciences/University of Colorado Boulder, Boulder, Colorado

^d Global Systems Laboratory, NOAA/OAR, Boulder, Colorado

(Manuscript received 8 August 2023, in final form 29 January 2024, accepted 31 January 2024)

ABSTRACT: Estimates of soil moisture from two National Oceanic and Atmospheric Administration (NOAA) models are compared to in situ observations. The estimates are from a high-resolution atmospheric model with a land surface model [High-Resolution Rapid Refresh (HRRR) model] and a hydrologic model from the NOAA Climate Prediction Center (CPC). Both models produce wetter soils in dry regions and drier soils in wet regions, as compared to the in situ observations. These soil moisture differences occur at most soil depths but are larger at the deeper depths below the surface (100 cm). Comparisons of soil moisture variability are also assessed as a function of soil moisture regime. Both models have lower standard deviations as compared to the in situ observations for all soil moisture regimes. The HRRR model's soil moisture is better correlated with in situ observations for drier soils as compared to wetter soils—a trend that was not present in the CPC model comparisons. In terms of seasonality, soil moisture comparisons vary depending on the metric, time of year, and soil moisture regime. Therefore, consideration of both the seasonality and soil moisture regime is needed to accurately determine model biases. These NOAA soil moisture estimates are used for a variety of forecasting and societal applications, and understanding their differences provides important context for their applications and can lead to model improvements.

SIGNIFICANCE STATEMENT: Soil moisture is an essential variable coupling the land surface to the atmosphere. Accurate estimates of soil moisture are important for forecasting near-surface temperature and moisture, predicting where clouds will form, and assessing drought and fire risks. There are multiple estimates of soil moisture available, and in this study, we compare soil moisture estimates from two different National Oceanic and Atmospheric Administration (NOAA) models to in situ observations. These comparisons include both soil moisture amount and variability and are conducted at several soil depths, in different soil moisture regimes, and for different seasons and years. This comprehensive assessment allows for an accurate assessment of biases within these models that would be missed when conducting analyses more broadly.

KEYWORDS: Soil moisture; Model evaluation/performance; Data assimilation; Land surface model; Seasonal cycle

1. Introduction

Knowledge of both soil moisture amount and variability is essential for many Earth system applications, such as forecasting near-surface temperature and moisture, predicting cloud formation, including convective initiation (e.g., Ek and Holtslag 2004), monitoring drought, flood, and fire risks (e.g., Svoboda et al. 2002; Rigden et al. 2020), and providing information for agricultural production (e.g., Madagari et al. 2017). As such, several advancements in the estimation and utilization of soil moisture have recently transpired. For example, in efforts to improve the accuracy of numerical weather prediction (NWP) and climate

models, model developers have focused on increasing the coupling between the land surface and atmosphere components of their data assimilation systems to eliminate persistent atmospheric prediction biases (e.g., Benjamin et al. 2022). Furthermore, NWP models are also beginning to explore the direct assimilation of new soil moisture observations (e.g., Carrera et al. 2019; Muñoz-Sabater et al. 2019; Lin and Pu 2020).

For these reasons, it is critical to understand the differences in the available soil moisture estimates from models and observations that are used in science, forecasting, and agricultural applications. Different estimates of soil moisture exist across the contiguous United States (CONUS), each with its own benefits and shortfalls. For example, in situ observations are often considered to be the most accurate and are therefore used as a benchmark. However, they have limited spatial coverage (e.g., Quiring et al. 2016). Other products, such as those from low-Earth-orbiting satellites, have lower temporal and spatial resolution (e.g., Liu et al. 2016). Soil moisture estimates from models depend on many assumptions and reflect the influence of observation-based data to different degrees (e.g., Smirnova et al. 1997; Huang et al. 1996; Mitchell et al. 2004). Several recent studies have made significant progress in comparing many of the available soil moisture estimates.

© Denotes content that is immediately available upon publication as open access.

© Supplemental information related to this paper is available at the Journals Online website: <https://doi.org/10.1175/WAF-D-23-0136.s1>

Corresponding author: Peter J. Marinescu, peter.marinescu@colostate.edu

For example, some studies have compared soil moisture temporal variability and memory between many large-scale land surface models (LSMs) and in situ soil monitoring networks across the CONUS, noting certain biases and uncertainties in the various estimates (e.g., Robock et al. 2003; Xia et al. 2014, 2015a; Dirmeyer et al. 2016; Wan et al. 2022). Other studies have extended soil moisture comparisons to include soil moisture retrievals from new satellite platforms (e.g., Shellito et al. 2016; Pan et al. 2016; Ford and Quiring 2019; Beck et al. 2021).

While various LSMs have been compared to in situ observations for several decades, these prior studies have primarily focused on models with horizontal resolutions on the scales of $1/8$ ° or larger (i.e., the North American Land Data Assimilation System models; Mitchell et al. 2004; Xia et al. 2012). Given the local, mesoscale variability of soil moisture processes and the subsequent impacts of soil moisture on atmospheric prediction (e.g., Koster et al. 2004; Taylor et al. 2011), high-resolution models should also be tested. Recently, Min et al. (2021) compared near-surface atmospheric and soil variables from the High-Resolution Rapid Refresh (HRRR) model (Dowell et al. 2022; James et al. 2022), which had a horizontal grid spacing of 3 km, to observations from the New York State Mesonet. They found that soil moisture was underestimated in HRRR, which contributed to warm and dry biases in atmospheric forecasts. Lee et al. (2023) compared many surface quantities in the HRRR model to in situ observations, including soil moisture, for the year of 2021. They reported that at 5–10 cm below the ground, HRRR dry soils had wet bias and wet soils had a dry bias, and when averaging over all locations in CONUS, the largest biases occurred in January–February 2021. While these two studies have provided initial assessments of HRRR soil moisture, there are many outstanding questions. For example, how well does the HRRR model capture the variability in soil moisture, as compared to in situ observations? Furthermore, do these soil moisture comparisons vary significantly over different time periods (e.g., seasons to years)? How do soil moisture estimates within 5 or 10 cm of the surface compare to those around 100 cm below the surface?

The goal of this study is a comprehensive evaluation of soil moisture estimates in NOAA models to in situ observing networks over a multiyear period. In particular, we include soil moisture estimates from the NOAA operational HRRR model, which utilizes the NOAA Rapid Update Cycle land surface model (RUC LSM; Smirnova et al. 1997) and have only recently been validated across CONUS in a systematic manner in the peer-reviewed literature (Lee et al. 2023). We also include the NOAA Climate Prediction Center (CPC) leaky-bucket hydrological model (Huang et al. 1996; van den Dool et al. 2003) and in situ observations from two nationwide networks: the NOAA/NCEI United States Climate Reference Network (USCRN; Bell et al. 2013) and the U.S. Department of Agriculture Soil Climate Analysis Network (SCAN; Schaefer et al. 2007). This work provides an assessment of the similarities and differences of soil moisture amounts and variability across three different products, which are all used in various operational and research applications.

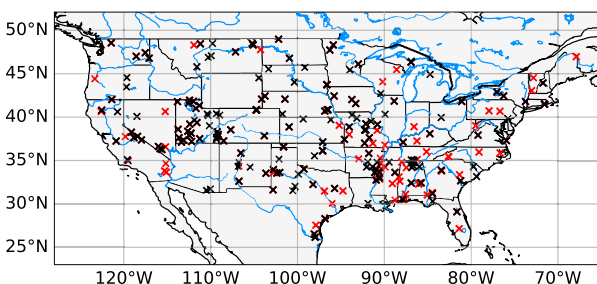


FIG. 1. In situ data locations (x marks) used for comparisons between in situ, HRRR, and CPC soil moisture amounts and variability. Black values represent in situ data that passed all quality control checks, while red values represent locations that did not pass error-variance-based quality control checks, as described in section 3b. Select major rivers and lakes are shown with blue lines.

2. Soil moisture data

a. In situ observations

The study uses in situ soil moisture observations from two nationwide networks. USCRN provides climate monitoring measurements of atmospheric and soil properties. To increase the coverage of the in situ observations, SCAN is also included. SCAN uses similar sensors to USCRN (i.e., Hydra Probe sensors) and typically have volumetric soil moisture (VSM; $\text{m}^3_{\text{water}} \text{m}^{-3}_{\text{soil}}$) measurements at the same soil depths (~ 5 , ~ 10 , ~ 20 , ~ 50 , and ~ 100 cm) as USCRN. Only data from these five levels are used for consistency. Dirmeyer et al. (2016) also found that these two networks have similar error variances. The observations represent point measurements of the soil moisture at specific sites across the United States. Daily data are used in this study and represent the average VSM of the entire 24-h period based on local standard time. The locations of these in situ observations are shown in Fig. 1.

b. HRRR model

The HRRR model is NOAA's operational, convection-allowing model, which has 3-km horizontal grid spacing and covers CONUS with a 1-h temporal refresh rate (Dowell et al. 2022; James et al. 2022). In this study, we use HRRRv3, which was operational between 12 July 2018 and 2 December 2020. The HRRR model utilizes a one-dimensional land surface model (RUC LSM; Smirnova et al. 1997), which predicts heat and moisture transfer vertically throughout the soil column. The RUC LSM has undergone several enhancements over the years, including increasing its resolution and incorporating new features, such as snow and ice models (Smirnova et al. 2000, 2016). The current version predicts VSM at nine vertical levels (0, 1, 4, 10, 30, 60, 100, 160, and 300 cm) and utilizes cycling of soil conditions over several years to better capture the soil moisture state. The HRRR utilizes moderately coupled land data assimilation, meaning that near-surface atmospheric data assimilation increments are used to adjust the soil analysis (e.g., Benjamin et al. 2022). Given the recent and continued development of the HRRR data assimilation system and land surface model, it is critical for assessments of HRRR's soil

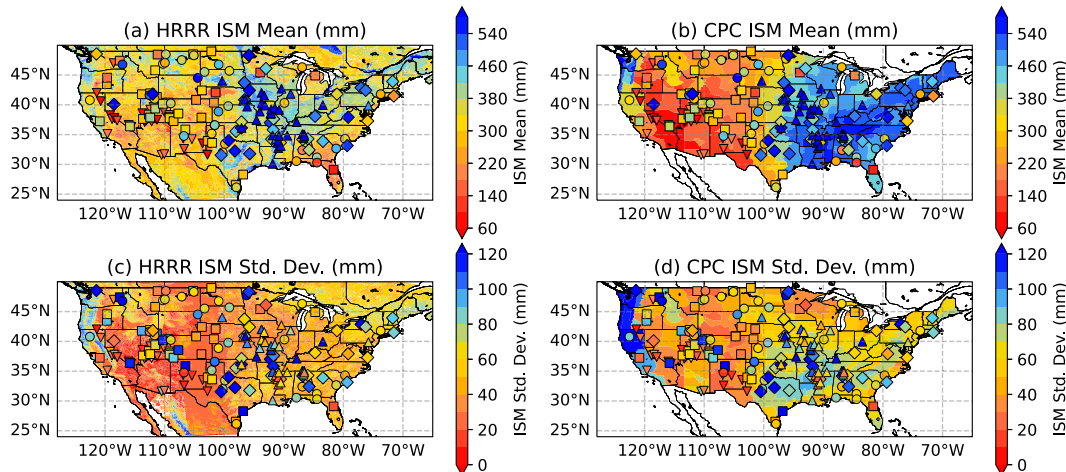


FIG. 2. The 1.6-m ISM mean amounts, temporally averaged over the study period for (a) the HRRR model and (b) the CPC model. (c),(d) As in (a) and (b), but for the 1.6-m ISM standard deviations. Filled symbols represent locations of the 172 in situ observations that pass all quality control checks, as described in the text, with the symbol color representing the in situ ISM mean or standard deviation, respectively. The symbols (∇ , \blacksquare , \bullet , \blacklozenge , \blacktriangle) represent the different soil moisture quintiles for 1.6-m ISM from the driest to wettest regimes, respectively.

moisture to other estimates. This study provides a benchmark for HRRR soil moisture estimates in support of the continued development of NOAA's land surface prediction capabilities in the Unified Forecast System (UFS; <https://ufscommunity.org>), which is a community-based, coupled Earth modeling system that is application-based to facilitate combining multiple forecast systems into a single forecast suite. The UFS is also designed to be the source system for NOAA operational applications. The focus of this study is on the analyzed soil moisture field (i.e., the model's initial conditions), rather than forecast fields, and thus our results are most directly relevant to the LSM and data assimilation system development.

c. CPC leaky-bucket model

The CPC soil moisture product utilizes a leaky-bucket model that solves the time tendency equation in soil moisture over a region from several inputs: precipitation minus evapotranspiration, net streamflow divergence and net groundwater loss (Huang et al. 1996; van den Dool et al. 2003). These inputs to the time tendency equation for soil moisture have been improved over the years with new observations and parameterizations (Fan and van den Dool 2004; Arevalo et al. 2021). The CPC model provides 1.6-m-deep integrated soil moisture (ISM; mm), and these estimates are provided daily for each of the NOAA climate divisions across the United States (Guttman and Quayle 1996). There are typically about 7–10 climate divisions per state, although there are fewer for states with smaller geographical areas, like those in the Northeast United States. The CPC soil moisture data are used as an input to the U.S. Drought Monitor (Svoboda et al. 2002) in addition to a suite of other tools,¹ and continues to be used as a reference dataset in various soil moisture application

studies, from assessing soil moisture impacts on carbon fluxes (e.g., Yao et al. 2021) to understanding climate impacts on agricultural production (e.g., Atiah et al. 2022).

3. Methods

a. In situ observations

Since the CPC product only provides 1.6-m ISM, VSM values from the in situ and HRRR data are vertically integrated in order to compare 1.6-m ISM in all three datasets. The VSM values are assumed to represent the mean value over a depth between the midpoints of the specified levels, as has been done in other studies (e.g., Dirmeyer et al. 2016; Ford and Quiring 2019). For example, the 10-cm VSM observation in the in situ data is assumed to represent the average VSM for the layer between 7.5 cm (i.e., the midpoint between 5 and 10 cm) and 15 cm (i.e., the midpoint between 10 and 20 cm). The 100-cm VSM in the in situ data is also assumed to be constant to the depth of 160 cm. The HRRR ISM calculations are better constrained than the in situ ISM calculations, since the HRRR VSM data span 3.0 m below ground using nine levels. VSM values are also compared between the HRRR and in situ data to glean whether certain vertical levels are driving the ISM differences between these two datasets. An understanding of soil moisture differences at varying depths is also critical since soil moisture's role in Earth system processes is depth dependent. In this study, comparisons are focused on 5-, 10-, and 100-cm depths. HRRR data, which is present at 4 and 10 cm below ground, is interpolated linearly to 5 cm for comparisons with in situ data at this depth. The surface layer in HRRR is also compared to the in situ data that is nearest to the surface (5-cm depth). In terms of spatial comparisons, the HRRR and CPC data are linearly interpolated to the locations of the in situ stations. The analysis is completed over a ~2.4-yr period from 12 July 2018 to 2 December 2020, which is the timeframe that

¹ <https://www.drought.gov/topics/soil-moisture>.

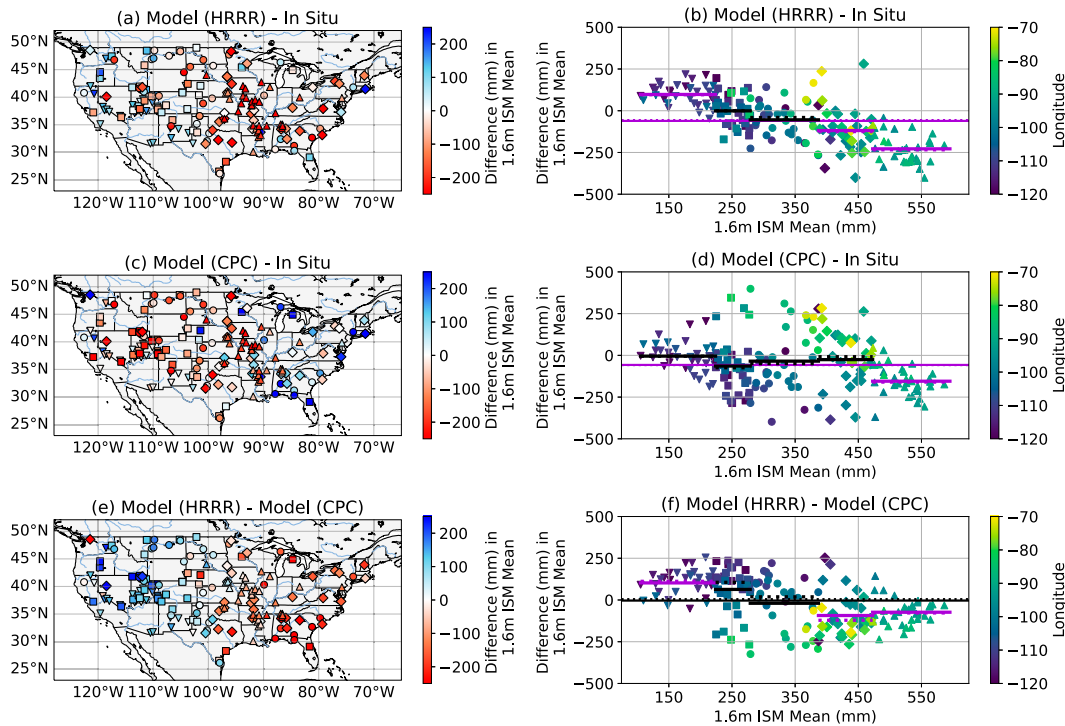


FIG. 3. Comparisons of the 1.6-m ISM mean differences between (a),(b) HRRR and in situ data; (c),(d) CPC and in situ data; and (e),(f) HRRR and CPC data. Note, (e) and (f) only show results from the same locations where in situ data are available for consistency. (left) Geographical space and (right) soil moisture space. The symbols (∇ , \blacksquare , \bullet , \blacklozenge , \blacktriangle) represent the different ISM quintiles from the driest to wettest regimes, respectively. In (b), (d), and (f), the horizontal solid and dashed lines represent the mean and median differences, respectively, for the entire dataset (longest line) and for the five soil moisture quintiles. Horizontal lines are colored purple if their associated mean differences pass statistical significance using a paired Student's t test at the 99.9th percentile.

HRRRv3 was operational. By confining the analyses to this time frame, uncertainties associated with model version changes are avoided.

b. Quality control

In situ data provide the most direct physical estimate of soil moisture, but it is important to ensure that the in situ data are of the highest quality. As such, a variety of quality control procedures are undertaken. First, in situ data are only included if they have VSM values available at all five vertical levels (~ 5 , ~ 10 , ~ 20 , ~ 50 , and ~ 100 cm), since missing data could lead to larger uncertainties in the ISM calculation. Second, in situ stations directly along the coast are removed due to unphysical spatial interpolations from the CPC and HRRR data. From the remaining in situ data (235 stations), we estimate the ratio of error variance to ISM variance using the method defined in Robock et al. (1995) and used in more recent soil moisture comparisons studies (e.g., Dirmeyer et al. 2016). In essence, soil moisture can be well approximated by a red-noise process (i.e., first-order Markov process; e.g., Delworth and Manabe 1988; Vinnikov and Yeserkepova 1991) with the natural logarithm of the soil moisture autocorrelation [$\ln(r)$] decreasing linearly with increased lag times (τ). For this study, autocorrelations are computed for τ of 1–30 days for each station's ISM daily

anomalies. A linear fit is applied to the $\ln(r)$ versus τ data and is extrapolated to $\tau = 0$. Deviations from 1 at $\tau = 0$ can be used to solve for the ratio of error variance to ISM variance (e.g., Robock et al. 1995). For this study, stations where this ratio is greater than 0.08 are removed. This error ratio threshold is inline with estimates of the mean error ratio of the USCRN and SCAN networks (Dirmeyer et al. 2016). While this error variance ratio threshold results in the removal of 63 ($\sim 27\%$) of the 235 available in situ stations, it provides more confidence that only the highest quality in situ observations are being used in the analyses. Even with the significant reduction of the in situ data, the stations span the entirety of the CONUS (Fig. 1). Different thresholds, autocorrelation lengths and dataset lengths were tested and did not qualitatively impact the results. Furthermore, statistical analyses with the dataset that did not include the error-variance-based quality control (235 stations) resulted in qualitatively similar results to those shown in this manuscript (see in the online supplemental material).

c. Quintile analysis

To determine whether differences in soil moisture estimates vary in different soil moisture regimes (i.e., wetter versus drier conditions), we composite the comparisons over locations with similar soil moisture amounts. The ISM or VSM values

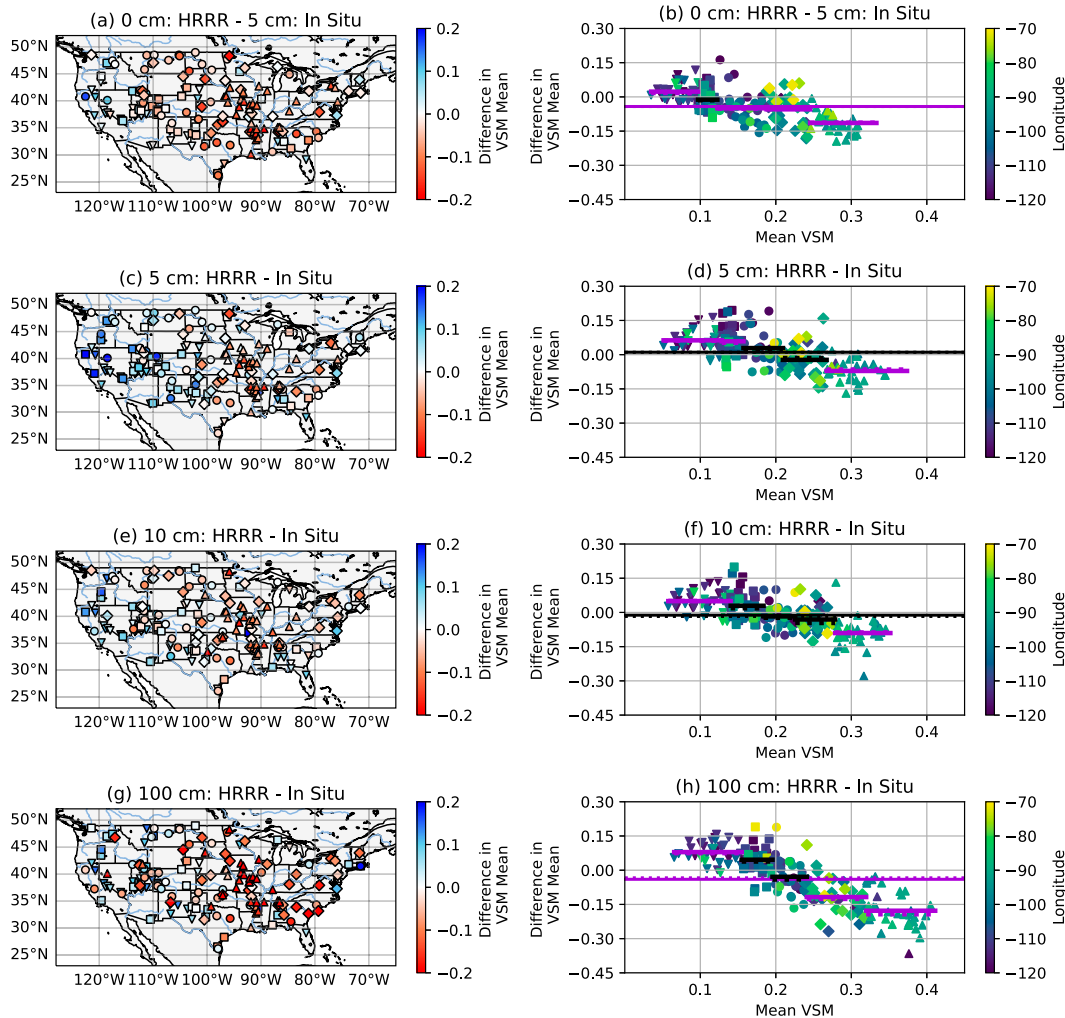


FIG. 4. Comparisons of the VSM mean differences between HRRR and in situ data at four different soil depths: (a),(b) surface in HRRR to 5 cm below ground in the in situ data; (c),(d) 5 cm below ground for both; (e),(f) 10 cm below ground for both; and (g),(h) 100 cm below ground for both. (left) Geographical space and (right) soil moisture space. The symbols (∇ , \blacksquare , \bullet , \blacklozenge , \blacktriangle) represent the different VSM quintiles from the driest to wettest regimes, respectively. In (b), (d), (f), and (h), the horizontal solid and dashed lines represent the mean and median differences, respectively, for the entire dataset (longest line) and for the five soil moisture quintiles. Horizontal lines are colored purple if their associated mean differences pass statistical significance using a paired Student's *t* test at the 99.9th percentile.

from each dataset are averaged temporally over the ~ 2.4 -yr study period for each location and are then averaged among the available datasets (i.e., all three datasets for ISM; the in situ and HRRR datasets for VSM). Using this mean, the locations are separated into five quintiles. For example, locations with a mean ISM estimate that is greater than or equal to the 0th percentile ISM and less than the 20th percentile ISM are placed in the lowest quintile of soil moisture amounts (i.e., driest locations). These locations are termed L_{00-20} . Similarly, locations that fall within the 20th–40th, 40th–60th, 60th–80th, and 80th–100th percentiles are termed L_{20-40} , L_{40-60} , L_{60-80} , and L_{80-100} , respectively, and represent dry to wet soil moisture regimes. There are either 34 or 35 stations included in

each of these quintiles. Stations within a quintile will often be located in similar regions across the United States (Fig. 2). For example, the intermountain west regions (longitudes between $\sim 100^{\circ}$ and $\sim 120^{\circ}$ W) are generally drier than other regions. Although, there are instances when stations that are located in proximity fall into very different quintiles, which are often due to local geographic features. For example, southern and central Utah have 1.6-m ISM mean values that fall into L_{00-20} or L_{20-40} , while northern Utah have 1.6-m ISM mean values that fall in L_{20-40} , L_{40-60} , or L_{60-80} , with the one L_{60-80} station being located right along the Cutler Reservoir and Bear River. Therefore, station that are located in similar regions may fall into very different soil moisture regimes. It is also important

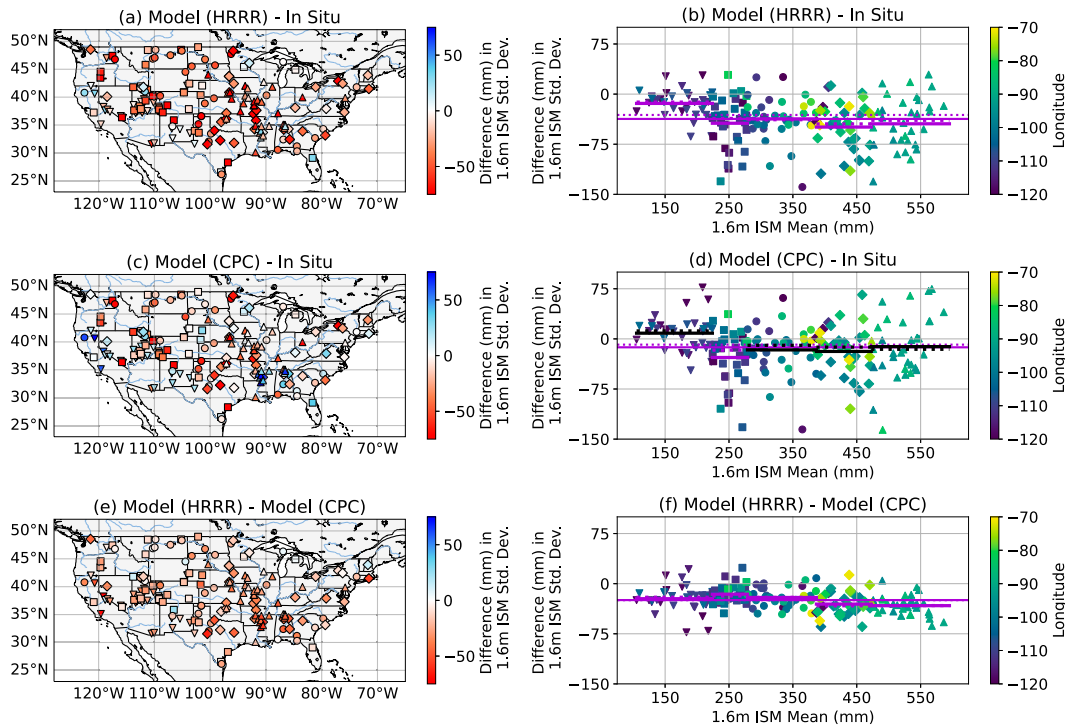


FIG. 5. Comparisons of the 1.6-m ISM standard deviation differences between (a),(b) HRRR and in situ data; (c),(d) CPC and in situ data; and (e),(f) HRRR and CPC data. Note, (e) and (f) only show results from the same locations where in situ data are available for consistency. (left) Geographical space and (right) soil moisture space. The symbols (∇ , \blacksquare , \bullet , \blacklozenge , \blacktriangle) represent the different ISM quintiles from the driest to wettest regimes, respectively. In (b), (d), and (f), the horizontal solid and dashed lines represent the mean and median differences, respectively, for the entire dataset (longest line) and for the five soil moisture quintiles. Horizontal lines are colored purple if their associated mean differences pass statistical significance using a paired Student's *t* test at the 99.9th percentile.

to note that different parts of the United States can have similar soil moisture amounts; for example, the Pacific Northwest and the Atlantic Northeast have similar 1.6-m ISM mean values and thus, fall into the same quintiles (Figs. 2a,b). The quintiles groupings allow for an assessment of whether there are systematic biases as a function of soil moisture, regardless of region or location. For clarity, we include maps for both ISM and VSM comparisons that show which stations fall into which quintiles in the following sections.

We assume that the station locations within each quintile represent a sample from the full population of locations within each quintile (i.e., soil moisture regime) across CONUS. Using the Student's *t* test, comparisons of the quintile sample means of soil moisture amounts and variability between the datasets can be used to determine whether the dataset differences are statistically significant (i.e., unlikely to be a result of random chance).

4. Soil moisture amount

a. ISM mean bias

Stark, regionally dependent mean differences are apparent in the ISM estimates (Figs. 2 and 3). The HRRR ISM values (Fig. 2a) have a more muted range than the CPC ISM values

(Fig. 2b). The HRRR ISMs are larger (i.e., wetter) than the CPC ISMs across the drier regions of CONUS (most of the western CONUS; Figs. 2a,b and 3e) and are smaller (i.e., drier) than the CPC ISMs in the wetter regions of CONUS (eastern half of CONUS and the coastal regions of the Pacific Northwest). These regional biases are associated with the varying soil moisture amounts in the different regions of CONUS.

When compared to both in situ ISM (Figs. 3a,b) and CPC ISM (Figs. 3e,f), HRRR is wetter in L_{00-20} (+101% and +97%, respectively, when taking the mean percentage bias for all locations in L_{00-20}) and drier in L_{80-100} (−34% and −13%, respectively). Therefore, while CPC also has a wet bias in the driest regimes, and a dry bias in the wettest regime, as compared to in situ observations, the CPC biases are significantly smaller than the HRRR biases. There are fewer moisture quintiles with statistically significant differences between the CPC and in situ ISM mean amounts, but this is a result of the middle three quintiles (L_{20-40} , L_{40-60} , L_{60-80}) having both positive and negative biases that results in a relatively small bias in the quintile mean (Fig. 3d). In fact, the CPC and in situ data have the largest differences among the dataset comparisons within these middle quintiles, which are clearly associated with specific geographic regions (Figs. 3c,d). For example, both L_{40-60} and L_{60-80} show minimal mean differences between the CPC and in situ ISMs, but at

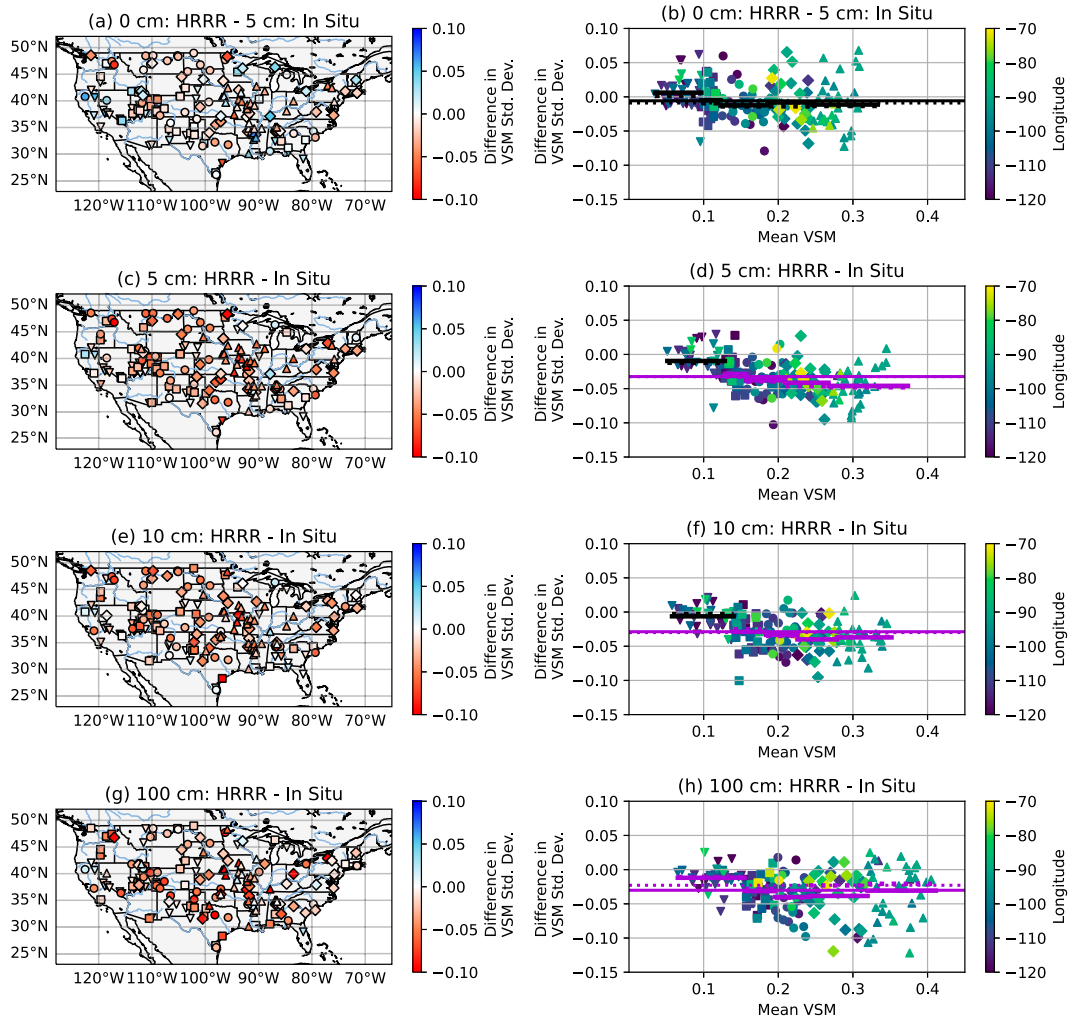


FIG. 6. Comparisons of the VSM standard deviation differences between HRRR and in situ data at four different soil depths: (a),(b) surface in HRRR to 5 cm below ground in the in situ data; (c),(d) 5 cm below ground for both; (e),(f) 10 cm below ground for both; and (g),(h) 100 cm below ground for both. (left) Geographical space and (right) soil moisture space. The symbols (∇ , \blacksquare , \bullet , \blacklozenge , \blacktriangle) represent the different VSM quintiles from the driest to wettest regimes, respectively. In (b), (d), (f), and (h), the horizontal solid and dashed lines represent the mean and median differences, respectively, for the entire dataset (longest line) and for the five soil moisture quintiles. Horizontal lines are colored purple if their associated mean differences pass statistical significance using a paired Student's t test at the 99.9th percentile.

eastern locations the CPC ISM means have a wet bias (Fig. 3d, green/yellow circles and diamonds) and at western locations the CPC ISM means have a dry bias (Fig. 3d, blue circles and diamonds), demonstrating that differences between the CPC and in situ ISM means are more dependent on geographic location and less dependent on soil moisture amount, as compared to the differences between the HRRR and in situ data. Note that we have also included mean absolute difference analyses in the supplemental material, which may be especially useful for these instances with both positive and negative biases in the same quintile. As is also shown in Fig. 2, Fig. 3 demonstrates both regional and soil-moisture-regime relationships to these ISM differences between the datasets

and thus, the potential shortfalls of conducting CONUS-wide means.

For some locations where CPC has very large differences from the in situ data, HRRR aligns more closely. These occurrences are typically associated with localized soil characteristics or topography, which are not captured in the coarser climate division regions used in the CPC product. For example, based on comparisons with the in situ ISM, the HRRR produces similarly dry soil moisture conditions within the Sand Hills region of Nebraska (e.g., red square at 42.1°N, 101.4°W in Fig. 2). The temporally averaged mean ISM for this location is 138 and 165 mm for the in situ and HRRR data, respectively, as compared to 372 mm in the CPC data (2–3 times larger).

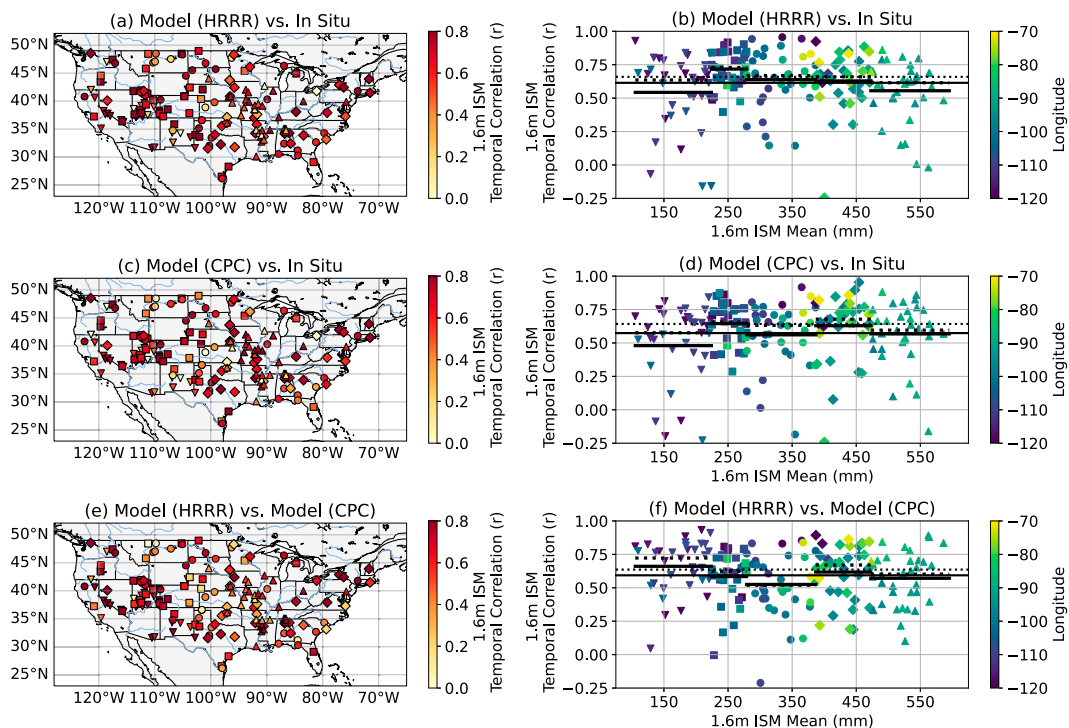


FIG. 7. Comparisons of 1.6-m ISM temporal correlation coefficients between (a),(b) HRRR and in situ data; (c),(d) CPC and in situ data; and (e),(f) HRRR and CPC data. Note, (e) and (f) only show results from the same locations where in situ data are available for consistency. (left) Geographical space and (right) soil moisture space. The symbols (∇ , \blacksquare , \bullet , \blacklozenge , \blacktriangle) represent the different ISM quintiles from the driest to wettest regimes, respectively. The horizontal solid and dashed lines represent the mean and median differences, respectively, for the entire dataset (longest line) and for the five soil moisture quintiles.

b. VSM mean comparisons at varying depths

To evaluate the depth dependence of soil moisture differences, the VSM data at different depths are compared in the HRRR and in situ data (Fig. 4). Since CPC only provides the 1.6-m integrated soil moisture, it is not included in the VSM analyses. Note, that the VSM data are also separated into quintiles from driest to wettest in a similar way to the ISM data, and this procedure is done for each vertical level. Therefore, in situ locations may fall into different quintiles for different vertical levels.

The same trend of the HRRR being wetter in L_{00-20} (i.e., the driest regions) and drier in L_{80-100} (i.e., the wettest regions) is present at all depths. This result is in-line with Lee et al. (2023), which recently found similar biases depending on soil moisture amount when comparing HRRR and USCRN at 5- and 10-cm depths for the year 2021. There are generally smaller differences in the middle quintiles, as compared to the wettest and driest regimes. At the lowest depths (100 cm below ground; Figs. 4g,h), the differences between the HRRR and in situ VSMs have larger magnitudes than shallower depths, especially for the driest and wettest regimes (L_{00-20} difference of +0.08 and L_{80-100} difference of -0.18). Near the surface (Figs. 4a,b), the driest 40% of the regions have relatively small differences (± 0.02), although significant dry biases are present for the wetter regions (-0.11). The

VSM data demonstrate that while the deeper soil layers (i.e., 100 cm below ground) are the primary drivers of the ISM trends, the shallower soil layers have similar trends.

5. Soil moisture variability

a. ISM standard deviation comparisons

Quantifying the variability (e.g., standard deviations and correlations) in soil moisture allows for an assessment on how models are capturing the magnitude and timing of soil moisture changes, as compared to in situ observations. Maps of the ISM standard deviations in the HRRR and CPC ISM data show similar patterns, with the highest variance occurring along the Pacific Northwest coast (Figs. 2c,d). The lowest ISM standard deviations occur along the Intermountain West and High Plains regions. In general, the HRRR ISMs have lower variance than the CPC data across the CONUS except for in the parts of the Rocky Mountains and in the Great Lakes and Northeast regions (Figs. 2c,d and 5e). HRRR produces larger spatial variability within the mountain and valley regions across the western United States that cannot be resolved in the CPC data.

The in situ observations generally have the highest ISM variance for most quintiles followed by CPC and HRRR, which has the lowest variances of the three datasets (Fig. 5).

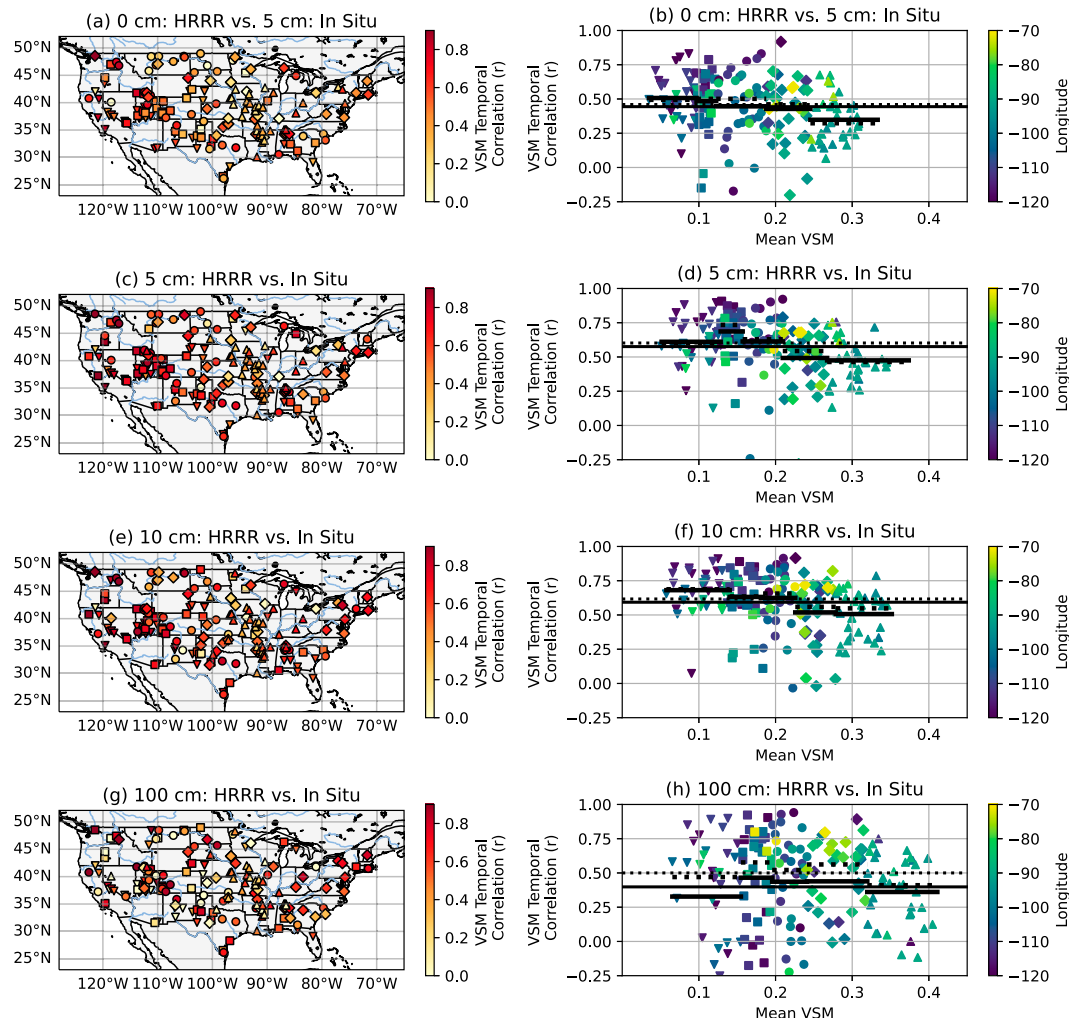


FIG. 8. Comparisons of the VSM temporal correlation coefficients between HRRR and in situ data at four different soil depths: (a),(b) surface in HRRR to 5 cm below ground in the in situ data; (c),(d) 5 cm below ground for both; and (e),(f) 10 cm below ground for both; and (g),(h) 100 cm below ground for both. (left) Geographical space and (right) soil moisture space. The symbols (∇ , \blacksquare , \bullet , \blacklozenge , \blacktriangle) represent the different VSM quintiles from the driest to wettest regimes, respectively. In (b), (d), and (f), the horizontal solid and dashed lines represent the mean and median differences, respectively, for the entire dataset (longest line) and for the five soil moisture quintiles.

The in situ and CPC quintile mean ISM standard deviations are not significantly different for most quintiles, while the HRRR quintile mean standard deviations are significantly lower for all quintiles when compared to both other datasets. Dirmeyer et al. (2016) showed that spatial scaling differences do not have a large impact ($\sim 10\%$) on in situ observation standard deviations via conducting tests where many stations that are separated by several kilometers to up to 100 km are averaged together. Therefore, the differences between the in situ and NOAA modeled standard deviations are likely due to other factors outside of dataset spatial scale differences, such as the representation of model processes or model input data. Furthermore, the large scatter in the ISM standard deviation differences (with both positive and negative differences) between the in situ data and both models (Figs. 5a–d) suggests that the cause of these differences may often be specific to a

station location. The differences between HRRR and CPC ISM standard deviations, however, demonstrate a systematic bias with less scatter between these two modeling frameworks (Figs. 5e,f).

b. VSM standard deviation comparisons at varying depths

VSM standard deviations at four different depths are compared between HRRR and in situ data (Fig. 6). Regardless of the soil moisture regime, the HRRR surface VSM standard deviations compare well to the 5-cm in situ observations in a mean sense, although there is more scatter in these comparisons than other levels (Figs. 6a,b). When averaging over all CONUS locations, the mean near-surface percentage differences in HRRR soil moisture from the in situ value is only -3.0% (Figs. 6a,b;

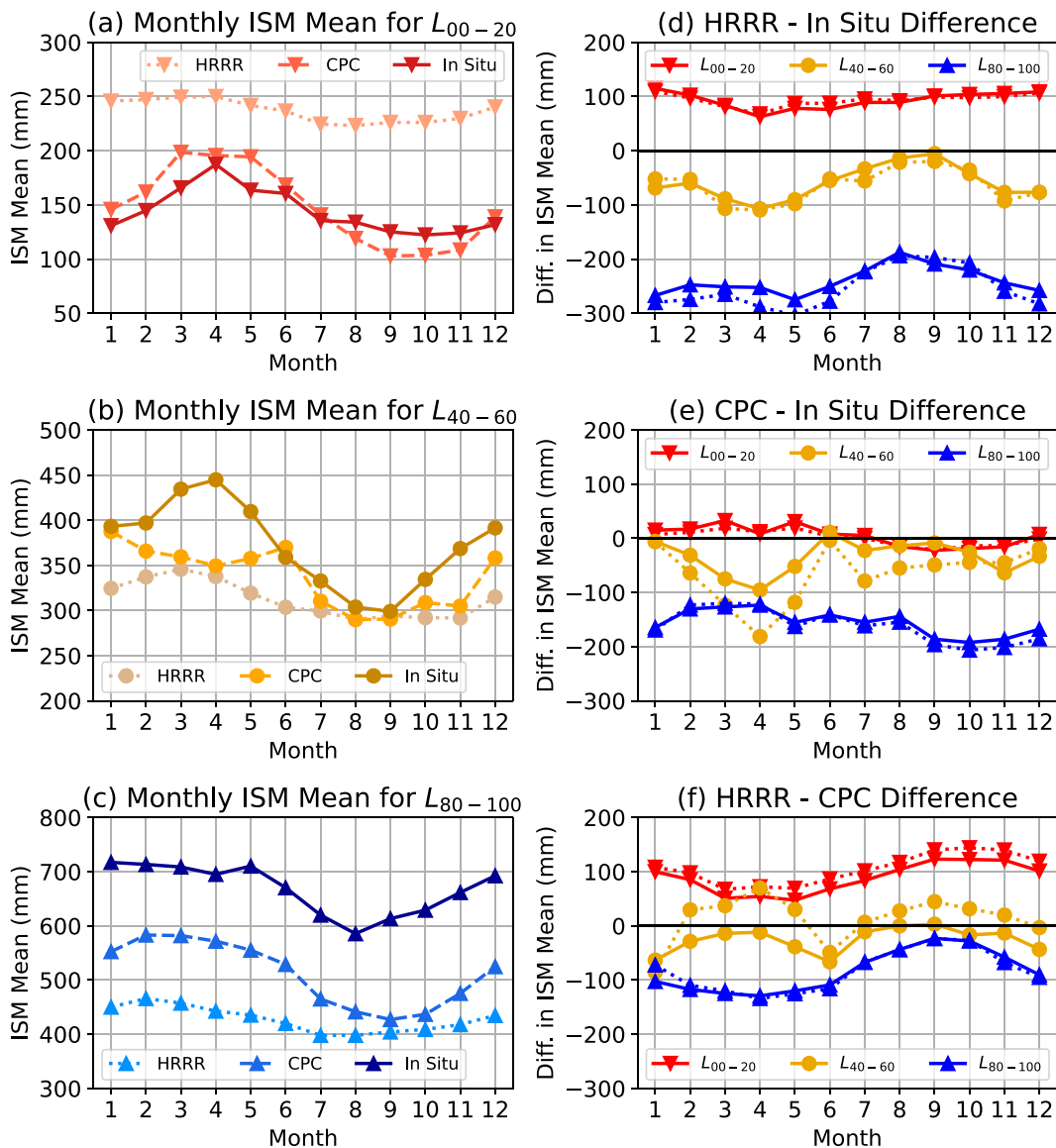


FIG. 9. (left) Monthly 1.6-m ISM means for HRRR, CPC, and in situ data for (a) L_{00-20} , (b) L_{40-60} , and (c) L_{80-100} . (right) Monthly mean (solid) and median (dashed) differences in ISM means for the three quintiles are shown for (d) HRRR minus in situ data, (e) CPC minus in situ data, and (f) HRRR minus CPC data.

longest, solid line). Larger standard deviations at the near-surface level in the HRRR model, as compared to lower levels, may be a result of improvements made in the HRRR's RUC LSM and the moderately coupled land data assimilation system that have been applied (Benjamin et al. 2022). However, at depths of 5 cm below ground and deeper (Figs. 6c–h), most quintiles have statistically significant differences in the standard deviations, in line with the ISM standard deviation differences between HRRR and in situ data (Figs. 5a,b). The mean percentage differences over all CONUS locations are -38.7% , -36.4% and -45.2% for the 5-, 10-, and 100-cm levels, respectively, with the HRRR always having lower standard deviations than the in situ datasets for every quintile. These

differences in VSM standard deviations are larger for wetter soil moisture regimes (L_{20-100}).

c. ISM temporal correlations

In addition to comparing standard deviations, temporal correlations over each station's time series over the entire time period are also compared among the datasets to determine how well the datasets vary together (Fig. 7). Depending on the station, these correlations included between 171 and 806 daily data points, with most stations (i.e., the median) having more than 737 daily data points. Because of the presence of outliers (Fig. 7), the focus is on median statistics. Comparing the entire datasets, the median correlation coefficient (r)

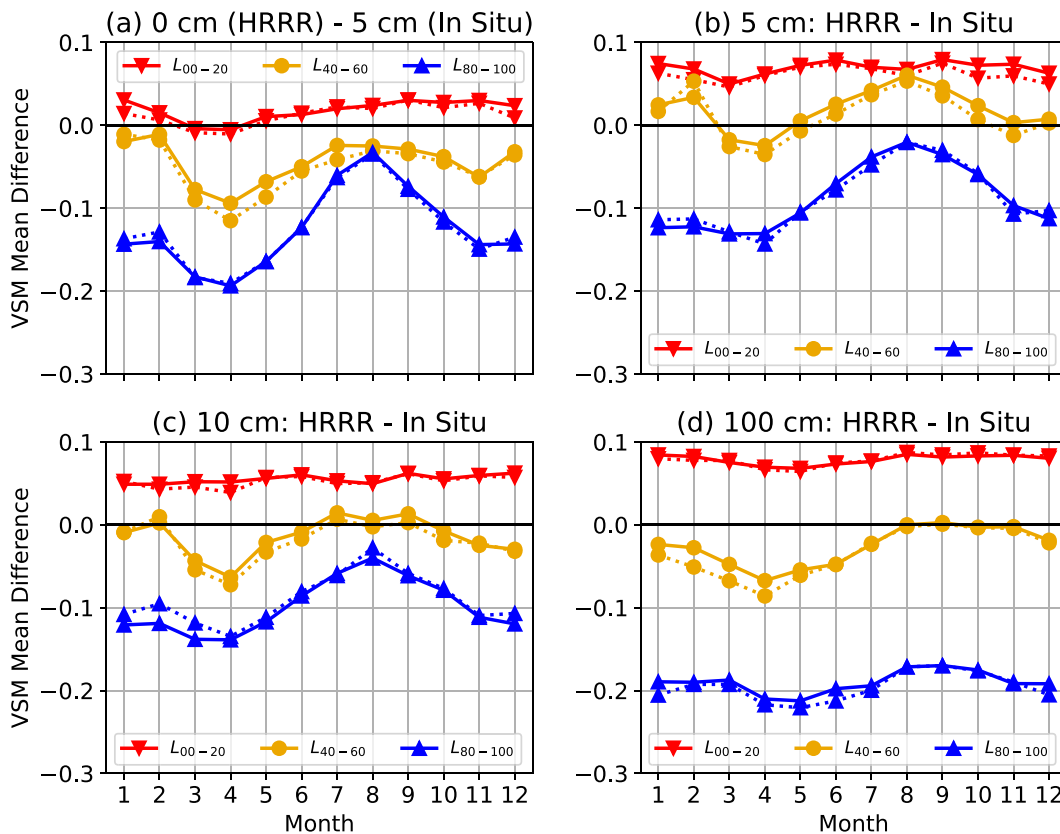


FIG. 10. Monthly mean (solid) and median (dashed) differences between HRRR and in situ VSM means ($\text{m}^3_{\text{water}} \text{m}^{-3}_{\text{soil}}$) at four different soil depths: (a) 0 cm in HRRR and 5 cm in the in situ data, (b) 5 cm for both, (c) 10 cm for both, and (d) 100 cm for both.

among the station locations are +0.66, +0.64, and +0.63 for the HRRR versus in situ data, the CPC versus in situ data, and the HRRR versus CPC data, respectively. While there is no clear trend in correlation as a function of soil moisture regime between the CPC and in situ datasets (Fig. 7b), the HRRR and in situ comparisons (Fig. 7a) show decreasing correlations with increasing soil moisture for all regimes except the driest regime (L_{00-20}). Thus, when compared to in situ observations, the HRRR model better captures the changes in soil moisture for drier regimes than wetter regimes, except for some of the driest locations. When comparing both the HRRR and CPC ISMs with the in situ data, the driest (L_{00-20}) and wettest (L_{80-100}) quintiles have the lowest correlations with the in situ data (medians between 0.58 and 0.64). Also, it is important to note that the northeast and northwest U.S. stations (Fig. 7) consistently have some of the best correlations among all three datasets.

d. VSM temporal correlations at varying depths

When assessing the varying soil moisture depths in the HRRR and in situ data, the highest correlations occur at the 5- and 10-cm depths (Figs. 8c–f). The median correlations for the entire dataset for the 5- and 10-cm levels are 0.60 and 0.62, respectively. These are much stronger correlations than when correlating the

100-cm levels ($r = 0.50$) and comparing the surface level in HRRR with the 5-cm level in the in situ data ($r = 0.46$). Note that the correlations of the surface level in HRRR to the 5-cm level in the in situ data are the lowest, while their standard deviations comparisons had the smallest mean differences (Fig. 6).

Importantly, regardless of depth, there is the same general trend of decreasing correlations for increasing soil moisture that is present in the ISM data. For example, for the 10-cm comparisons, L_{00-20} have temporal correlations of 0.69, while L_{80-100} have temporal correlations of 0.55. These results show that the trends in ISM temporal correlations between HRRR and in situ datasets (Figs. 7a,b) are generally consistent for all soil depths presented in this study.

6. Seasonal and annual variability

a. Mean ISM and VSM seasonality

The following sections show results where these same statistics (mean differences, standard deviation differences, correlations) are calculated based on data for each month during the ~2.4-yr study period in order to assess whether differences between the datasets have seasonal variability. Figure 9 shows the 1.6-m ISM for the driest (L_{00-20} , Fig. 9a), middle (L_{40-60} , Fig. 9b), and wettest (L_{80-100} , Fig. 9c) soil moisture

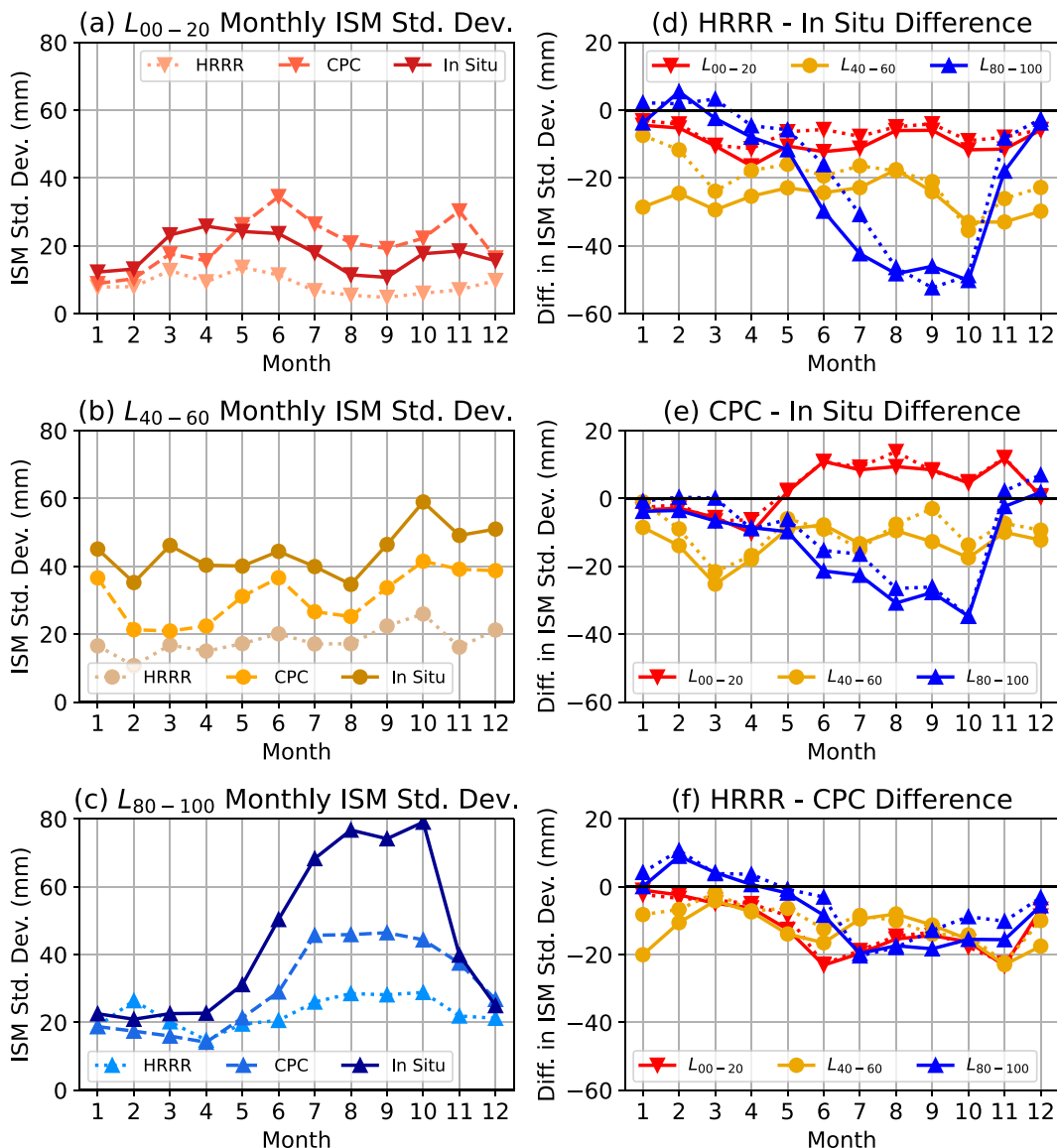


FIG. 11. (left) Monthly 1.6-m ISM standard deviations for HRRR, CPC, and in situ data for (a) L_{00-20} , (b) L_{40-60} , and (c) L_{80-100} . (right) Monthly mean (solid) and median (dashed) ISM standard deviation differences for the three quintiles are shown for (d) HRRR minus in situ data, (e) CPC minus in situ data, and (f) HRRR minus CPC data.

regimes as a function of month for all three datasets, including the monthly differences (Figs. 9d–f) between the datasets. Generally, both the HRRR and CPC models capture the timing of the maximum and minimum ISMs that occur in the in situ data. For the driest regimes (Fig. 9a), the CPC and in situ locations are much more in-line, with the HRRR values overestimating soil moisture throughout the year with the largest biases occurring in the fall and winter months (Figs. 9a,d). For L_{40-60} , both the CPC and HRRR models underestimate ISM by ~ 50 –100 mm in the March–May period and are closer to the in situ data during the July–September time period (Fig. 9b). Finally, for the wettest locations (L_{80-100} ; Fig. 9c), both HRRR and CPC have low ISM biases compared to the in situ data

throughout the year, but the timing of largest and smallest biases varies between the comparisons.

When assessing the HRRR and in situ monthly comparisons over the different VSM depths (Fig. 10), similar seasonal trends in soil moisture biases are present at all depths. Furthermore, the differences in the VSM mean biases at shallower levels have stronger seasonal changes than at the deepest level. For the driest regions (L_{00-20}), the best comparisons occur in the first half of the year, with the best-performing month depending on the depth. The worst comparisons for L_{00-20} occur in the second half of the year. For the wettest regions (L_{80-100}), the worst comparisons are generally in March–May, and the best comparisons are in August–October. Generally, the timing of these

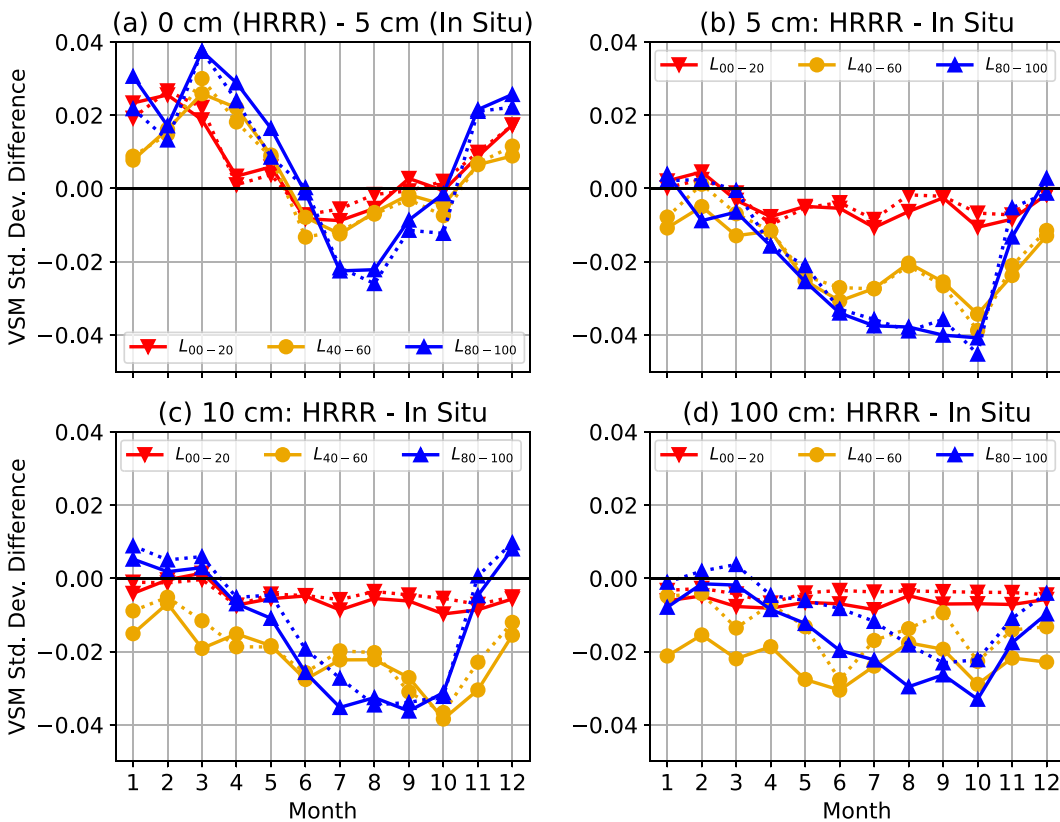


FIG. 12. Monthly mean (solid) and median (dashed) differences between HRRR and in situ VSM standard deviations ($\text{m}^3 \text{water} \text{m}^{-3}$) at four different soil depths: (a) 0 cm in HRRR and 5 cm in the in situ data, (b) 5 cm, (c) 10 cm, and (d) 100 cm.

peaks and troughs in the comparisons are consistent among the different soil moisture depths. It is important to note that Lee et al. (2023) found that when averaging across all stations, there is minimal bias from May to November with larger biases in January–February at the 5- and 10-cm levels. However, when separating the data into the different soil moisture regimes, the January–February bias reported by Lee et al. (2023) is likely caused by the larger negative biases in the wettest soil moisture regimes (L_{80-100}), which more than offsets the smaller magnitude positive biases in the drier regimes (e.g., L_{00-20}). During May–November, significant biases are still present for the different soil moisture regimes, but these differences better balance when averaging over all of the CONUS regions, resulting in smaller CONUS-wide biases during this time period.

b. Mean ISM and VSM standard deviation seasonality

Similar to the ISM monthly mean values, both the HRRR and CPC models produce similar seasonal cycles for ISM standard deviations as compared to the in situ data in terms of the timing of peaks and troughs (Figs. 11a–c). Both HRRR and CPC underpredict standard deviations of ISMs throughout the year for all soil moisture regimes, except for the CPC during the June–November period for the driest regime (L_{00-20} , Fig. 11e), and HRRR during January–March for the wettest regimes (L_{80-100}).

When comparing the 5-, 10-, and 100-cm soil moisture depths for the HRRR and in situ data (Figs. 12b–d), the worst comparisons occur in the May–November time period, regardless of soil moisture regime, except for the deepest levels of the drier regimes (Fig. 12d; L_{00-20} and L_{40-60}), which have less seasonality in the comparisons. For most of the data, the comparisons of soil moisture standard deviations between HRRR and in situ data show minimal differences in the months of December–March, with the worst comparisons during this time period for L_{40-60} . Note that while the comparisons at the surface in HRRR to in situ 5-cm depth had relatively low standard deviation differences (Figs. 6a,b), there are larger positive and negative biases in different times of the year (Fig. 12a) that offset each other when not considering this seasonal variability.

c. ISM and VSM temporal correlation seasonality

For the driest regimes (L_{00-20} , red lines in Fig. 13), the temporal correlations between both models and the in situ data (Figs. 13a,b) are generally lowest in the January–February and July–September periods and are highest in the March–June period. Both the HRRR and CPC models also perform similar when being compared to the in situ data for the wettest regimes, with the best correlations occurring in October (mean and median $r > 0.6$), and the worst comparisons

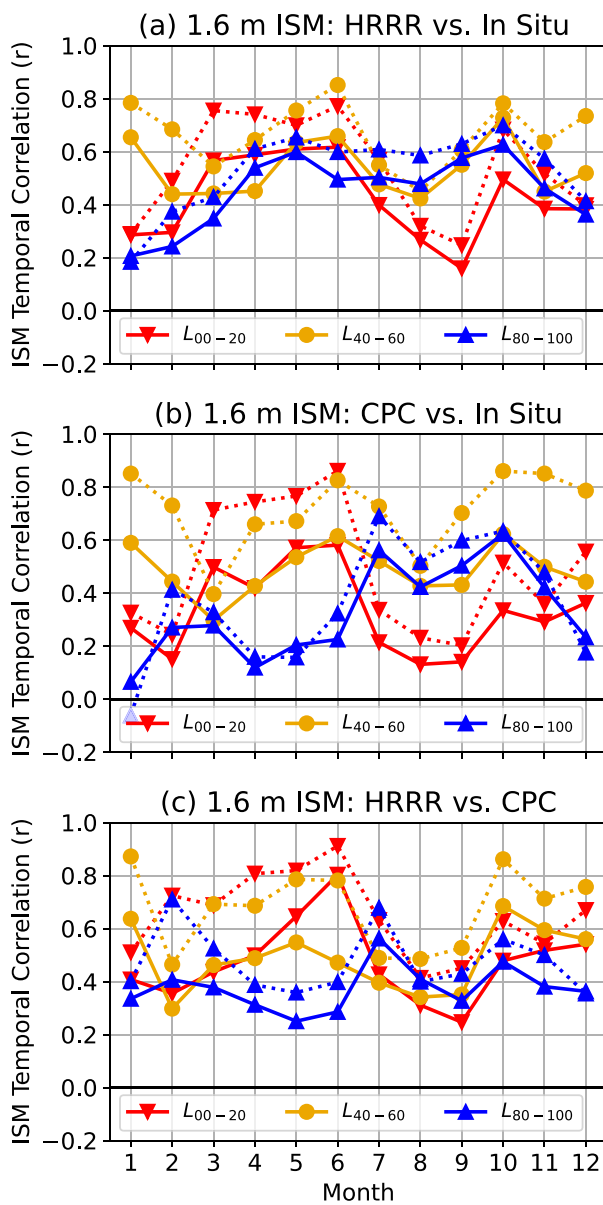


FIG. 13. Monthly 1.6-m ISM mean (solid) and median (dashed) temporal correlation coefficients for L_{00-20} , L_{40-60} , and L_{80-100} between (a) HRRR and in situ data, (b) CPC and in situ data, and (c) HRRR and CPC data.

occurring in December and January. The CPC correlations with the in situ data are lower than the HRRR correlations with the in situ data for most times of the year. The consistencies between both modeling platforms comparisons with the in situ data, in terms of best and worst performing time periods, may suggest periods of relatively high and low ISM predictability.

In terms of the different depth comparisons between the HRRR and in situ correlations, the 100-cm depth generally has the poorest temporal correlations for all times of the year (Fig. 14d), especially for the wettest regime (L_{80-100}). Comparisons nearer to the surface (Figs. 14a–c) generally depict

similar seasonal cycles regardless of depth, with the 5- and 10-cm depth comparisons (Figs. 14b,c) having the strongest correlations. For the wetter soil moisture regimes (L_{40-60} and L_{80-100}), the near-surface, 5- and 10-cm temporal correlations have similar seasonal trends, with the highest correlations from May to October and lowest correlations from January to April. For the driest regime (L_{00-20}), the near-surface, 5-cm, and 10-cm correlations also have similar seasonal cycles, with the worst performing months being January and August through September. These are generally in-line with the ISM temporal correlations (Fig. 13a). While the 100-cm depth has similar seasonal cycles to the shallower depths, there are some months with significant differences between the deep and shallow soil moisture correlations (i.e., May for L_{80-100}). Note that the median correlations results have higher correlations than the mean, especially at the 100-cm depth, showing the impact of outlier station results at these deep soil levels.

d. Interannual variability

Because of the length of these analyses (~2.4 years), an assessment of the consistency of the statistics presented can be shown for two different years. Each statistic (mean bias, standard deviation bias, and temporal correlations) are compared for two different year-long time periods (1 December 2018–2019 and 1 December 2019–2020; not shown), and the qualitative conclusions that are drawn from the analyses presented in this study do not change in the two individual analysis years. Furthermore, the VSM mean bias results are in line with the results presented in Lee et al. (2023), which focused on a separate year that was not included in this study (2021), further demonstrating the robustness of these results. It is important to note that soil moisture biases may vary on time scales longer than that which can be assessed with the ~2.4-yr dataset used in this study. Recall, this ~2.4-yr dataset was coincident with the operational HRRRv3 and used in order to avoid biases introduced by using different model versions. Additional research with longer datasets would be needed for determining the interannual variability of these dataset comparisons.

7. Conclusions

A comparison of 1.6-m integrated soil moisture (ISM) across the continental United States (CONUS) between two different NOAA soil moisture modeling frameworks with in situ observations is conducted, including comparisons of both mean soil moisture amount and variability. This analysis includes the HRRR model with its RUC LSM, the CPC leaky-bucket model and in situ observations from two national networks. The same comparisons of volumetric soil moisture (VSM) at several soil moisture depths (near-surface and 5, 10, and 100 cm below the ground) between HRRR and in situ data are also conducted to assess the consistency of soil moisture comparisons at different depths. Soil moisture amount and variability are compared as a function of soil moisture regime, geographical location, and time of year to provide a comprehensive

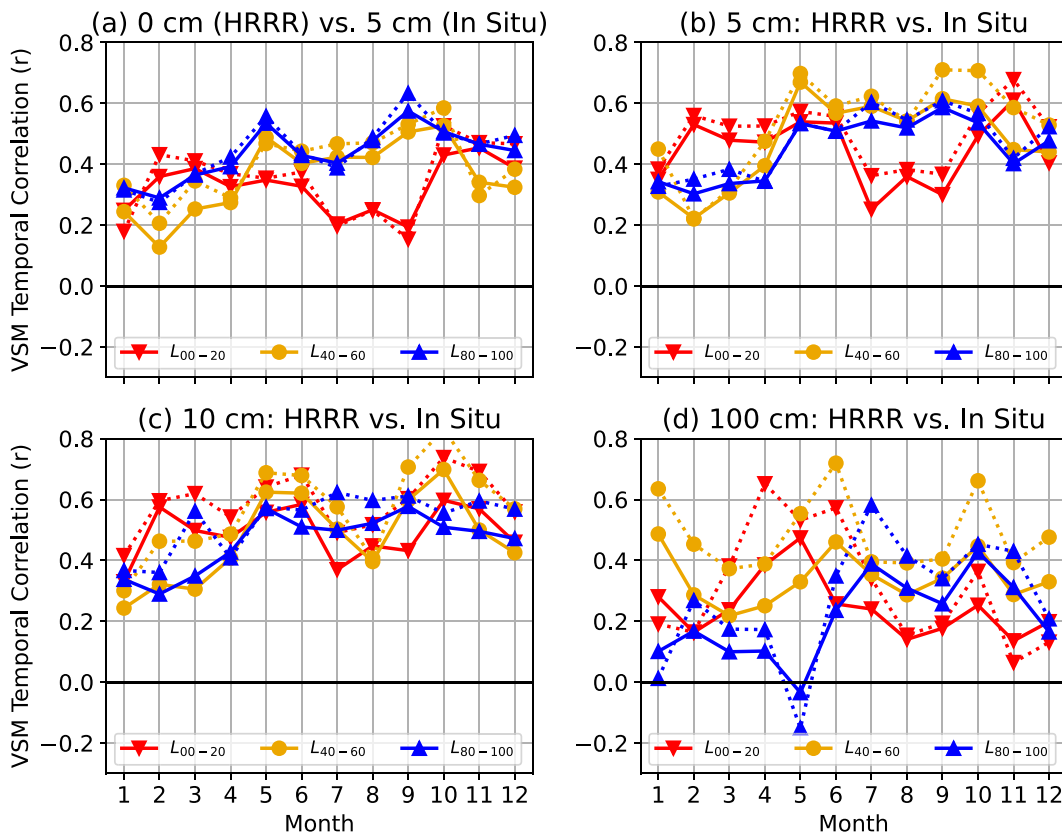


FIG. 14. Monthly VSM mean (solid) and median (dashed) temporal correlation coefficients between HRRR and in situ data for L_{00-20} , L_{40-60} , and L_{80-100} . Comparisons are shown for four different soil depths (a) 0 cm in HRRR and 5 cm in the in situ data, (b) 5 cm in both, (c) 10 cm in both, and (d) 100 cm in both.

assessment. These soil moisture data are used in many operational and research applications, including atmospheric forecasting, drought and agricultural crop monitoring, and assessing flood and fire risks. Therefore, quantifying differences in these NOAA models to observational networks across CONUS is critical.

Several conclusions are drawn from these comparisons.

- 1) The HRRR and CPC ISMs are both larger (i.e., wetter) in the driest regions and smaller (i.e., drier) in the wettest regions, as compared to in situ observations. These results are in-line with a comparison of HRRR VSM with in situ observations recently conducted by Lee et al. (2023).
- 2) All depths show the trend of a dry bias in wetter regimes and a wet bias in drier regimes in HRRR compared to in situ observations, but the biases are smaller at shallower depths.
- 3) CPC ISM differences from in situ data are more related to specific geographic regions and less related to soil moisture regimes. HRRR differences from in situ data have a clearer trend as a function of soil moisture regime that is less dependent on geographical location.
- 4) The in situ observations have the largest ISM standard deviations, followed by the CPC leaky-bucket model and the

HRRR model. The HRRR data has significantly smaller ISM standard deviations than both other datasets for every soil moisture regime.

- 5) Both ISM and VSM temporal correlations between HRRR and in situ data generally decrease with increasing soil moisture, suggesting better HRRR performance in drier regimes, in terms of capturing changes in soil moisture that concurrently match in situ observations; although some stations along the northeastern and northwestern CONUS coasts have relatively wet soils and have some of the highest correlations, and some of the driest locations have low correlations at the deepest soil depths.
- 6) There is significant seasonal variability in soil moisture comparisons that can vary based on the soil moisture regime. Therefore, it is important to consider both the seasonality and soil moisture regime when quantifying differences between modeled estimates and observations of soil moisture.

In terms of modeled soil moisture, biases in the input datasets (i.e., precipitation or radiation), whether they come from a coupled atmospheric model in the case of HRRR or external sources in the case of CPC, have been shown to lead to biases in land surface model calculations (e.g., Mitchell et al. 2004; Min et al. 2021). Choices in the land surface model structure and parameterizations, such as the number and thickness of soil layers,

the representation of soil and vegetation, and other model parameters, can also lead to biases in soil moisture prediction (e.g., Mitchell et al. 2004; Xia et al. 2014, 2015b). Min et al. (2021) found that snowmelt, freezing/thawing, and/or biases in precipitation and evapotranspiration led to differences in HRRR soil moisture as compared to in situ observations in New York and that the most relevant processes causing these differences varied throughout the year. These prior works demonstrate that there are many combinations of error sources for soil moisture prediction, which can vary for different locations. The results in this study demonstrate that there are biases in NOAA modeled soil moisture amounts and variability as compared to in situ observations across CONUS and that these biases are dependent on the soil moisture regime, the specific location, and the time of year. As such, future research should focus on understanding the model processes that are causing these biases through systematic modeling experiments that can better assess the impacts of the many assumptions within land surface modeling. Our results show specific soil moisture regimes, locations and/or times of the year with larger biases (e.g., both the wettest and driest regimes) that should be the focus of additional research.

These results also provide important context to the current users of these models and observations. For example, HRRR's land data assimilation system has recently undergone changes that primarily impact the near-surface soil state (Benjamin et al. 2022). The comparisons presented may provide a first step toward understanding the impact of these model changes. Furthermore, these results can assist with the continued development and refinement of soil moisture models and products. The analyses presented here were motivated by preparing training and validation data for a machine learning algorithm that uses data from the Advanced Baseline Imager on board NOAA's Geostationary Operational Environmental Satellite to estimate the soil moisture state at very high resolution (i.e., on the order of ~ 1 km). With a recent focus on land-atmosphere coupling and a continued shift toward higher-resolution models, such a product could be used as a supplementary input for strongly coupled land atmosphere data assimilation in the next generation of atmospheric models. Understanding our current estimates of soil moisture and their differences is an important first step for improving these estimates and land surface modeling.

Acknowledgments. This work was supported by the NOAA FY21 High Performance Computing and Communications Program's Information Technology Incubator. We would also like to acknowledge helpful feedback on and interest in this work from Tanya Smirnova, Stan Benjamin, Curtis Alexander, and Eric James.

Data availability statement. Several in situ and model datasets are used in this study. The USCRN data (Palecki et al. 2013) and the SCAN data (SCAN 2016) used in this study are publicly available. The daily CPC data are available via anonymous FTP from [ftp.cpc.ncep.noaa.gov/wd51yf/us/w_daily/](ftp://cpc.ncep.noaa.gov/wd51yf/us/w_daily/). The HRRR operational model data (HRRRv3) is stored and

accessed via the NOAA Hera supercomputer and is publicly archived at either <https://registry.opendata.aws/noaa-hrrr-pds/> or <https://console.cloud.google.com/marketplace/product/noaa-public/hrrr>. The code used to generate the analyses and figures in this manuscript are available on GitHub via <https://doi.org/10.5281/zenodo.10553502> (Marinescu 2024).

REFERENCES

Arevalo, J., J. Welty, Y. Fan, and X. Zeng, 2021: Implementation of snowpack treatment in the CPC water balance model and its impact on drought assessment. *J. Hydrometeor.*, **22**, 1235–1247, <https://doi.org/10.1175/JHM-D-20-0201.1>.

Atiah, W. A., L. K. Amekudzi, R. A. Akum, E. Quansah, P. Antwi-Agyei, and S. K. Danuor, 2022: Climate variability and impacts on maize (*Zea mays*) yield in Ghana, West Africa. *Quart. J. Roy. Meteor. Soc.*, **148**, 185–198, <https://doi.org/10.1002/qj.4199>.

Beck, H. E., and Coauthors, 2021: Evaluation of 18 satellite- and model-based soil moisture products using in situ measurements from 826 sensors. *Hydrol. Earth Syst. Sci.*, **25**, 17–40, <https://doi.org/10.5194/hess-25-17-2021>.

Bell, J. E., and Coauthors, 2013: U.S. climate reference network soil moisture and temperature observations. *J. Hydrometeor.*, **14**, 977–988, <https://doi.org/10.1175/JHM-D-12-0146.1>.

Benjamin, S. G., T. G. Smirnova, E. P. James, L.-F. Lin, M. Hu, D. D. Turner, and S. He, 2022: Land–snow data assimilation including a moderately coupled initialization method applied to NWP. *J. Hydrometeor.*, **23**, 825–845, <https://doi.org/10.1175/JHM-D-21-0198.1>.

Carrera, M. L., B. Bilodeau, S. Bélaire, M. Abrahamowicz, A. Russell, and X. Wang, 2019: Assimilation of passive L-band microwave brightness temperatures in the Canadian Land Data Assimilation System: Impacts on short-range warm season numerical weather prediction. *J. Hydrometeor.*, **20**, 1053–1079, <https://doi.org/10.1175/JHM-D-18-0133.1>.

Delworth, T. L., and S. Manabe, 1988: The influence of potential evaporation on the variabilities of simulated soil wetness and climate. *J. Climate*, **1**, 523–547, [https://doi.org/10.1175/1520-0442\(1988\)001<0523:TIOPEO>2.0.CO;2](https://doi.org/10.1175/1520-0442(1988)001<0523:TIOPEO>2.0.CO;2).

Dirmeyer, P. A., and Coauthors, 2016: Confronting weather and climate models with observational data from soil moisture networks over the United States. *J. Hydrometeor.*, **17**, 1049–1067, <https://doi.org/10.1175/JHM-D-15-0196.1>.

Dowell, D. C., and Coauthors, 2022: The High-Resolution Rapid Refresh (HRRR): An hourly updating convection-allowing forecast model. Part I: Motivation and system description. *Wea. Forecasting*, **37**, 1371–1395, <https://doi.org/10.1175/WAF-D-21-0151.1>.

Ek, M. B., and A. A. M. Holtslag, 2004: Influence of soil moisture on boundary layer cloud development. *J. Hydrometeor.*, **5**, 86–99, [https://doi.org/10.1175/1525-7541\(2004\)005<0086:IOSMOB>2.0.CO;2](https://doi.org/10.1175/1525-7541(2004)005<0086:IOSMOB>2.0.CO;2).

Fan, Y., and H. van den Dool, 2004: Climate Prediction Center global monthly soil moisture data set at 0.5° resolution for 1948 to present. *J. Geophys. Res.*, **109**, D10102, <https://doi.org/10.1029/2003JD004345>.

Ford, T. W., and S. M. Quiring, 2019: Comparison of contemporary in situ, model, and satellite remote sensing soil moisture with a focus on drought monitoring. *Water Resour. Res.*, **55**, 1565–1582, <https://doi.org/10.1029/2018WR024039>.

Guttman, N. B., and R. G. Quayle, 1996: A historical perspective of U.S. climate divisions. *Bull. Amer. Meteor. Soc.*, **77**, 293–303, [https://doi.org/10.1175/1520-0477\(1996\)077<0293:AHPOUC>2.0.CO;2](https://doi.org/10.1175/1520-0477(1996)077<0293:AHPOUC>2.0.CO;2).

Huang, J., H. M. Van Den Dool, and K. P. Georgakakos, 1996: Analysis of model-calculated soil moisture over the United States (1931–1993) and applications to long-range temperature forecasts. *J. Climate*, **9**, 1350–1362, [https://doi.org/10.1175/1520-0442\(1996\)009<1350:AOMCSM>2.0.CO;2](https://doi.org/10.1175/1520-0442(1996)009<1350:AOMCSM>2.0.CO;2).

James, E. P., and Coauthors, 2022: The High-Resolution Rapid Refresh (HRRR): An hourly updating convection-allowing forecast model. Part II: Forecast performance. *Wea. Forecasting*, **37**, 1397–1417, <https://doi.org/10.1175/WAF-D-21-0130.1>.

Koster, R. D., and Coauthors, 2004: Regions of strong coupling between soil moisture and precipitation. *Science*, **305**, 1138–1140, <https://doi.org/10.1126/science.1100217>.

Lee, T. R., R. D. Leeper, T. Wilson, H. J. Diamond, T. P. Meyers, and D. D. Turner, 2023: Using the U.S. climate reference network to identify biases in near- and subsurface meteorological fields in the High-Resolution Rapid Refresh (HRRR) weather prediction model. *Wea. Forecasting*, **38**, 879–900, <https://doi.org/10.1175/WAF-D-22-0213.1>.

Lin, L.-F., and Z. Pu, 2020: Improving near-surface short-range weather forecasts using strongly coupled land–atmosphere data assimilation with GSI-EnKF. *Mon. Wea. Rev.*, **148**, 2863–2888, <https://doi.org/10.1175/MWR-D-19-0370.1>.

Liu, J., X. Zhan, C. Hain, J. Yin, L. Fang, Z. Li, and L. Zhao, 2016: NOAA Soil Moisture Operational Product System (SMOPS) and its validations. *2016 IEEE Int. Geoscience and Remote Sensing Symp. (IGARSS)*, Beijing, China, Institute of Electrical and Electronics Engineers, 3477–3480, <https://doi.org/10.1109/IGARSS.2016.7729899>.

Madadgar, S., A. AghaKouchak, A. Farahmand, and S. J. Davis, 2017: Probabilistic estimates of drought impacts on agricultural production. *Geophys. Res. Lett.*, **44**, 7799–7807, <https://doi.org/10.1002/2017GL073606>.

Marinescu, P. J., 2024: pjmarinescu/CIRA_Soil_Moisture: CIRA_Soil_Moisture_Project_v2.0 (version 2.0). Zenodo, accessed 22 January 2024, <https://doi.org/10.5281/zenodo.10553502>.

Min, L., D. R. Fitzjarrald, Y. Du, B. E. J. Rose, J. Hong, and Q. Min, 2021: Exploring sources of surface bias in HRRR using New York State mesonet. *J. Geophys. Res. Atmos.*, **126**, e2021JD034989, <https://doi.org/10.1029/2021JD034989>.

Mitchell, K. E., and Coauthors, 2004: The multi-institution North American Land Data Assimilation System (NLDAS): Utilizing multiple GCIP products and partners in a continental distributed hydrological modeling system. *J. Geophys. Res.*, **109**, D07S90, <https://doi.org/10.1029/2003JD003823>.

Muñoz-Sabater, J., H. Lawrence, C. Albergel, P. Rosnay, L. Isaksen, S. Mecklenburg, Y. Kerr, and M. Drusch, 2019: Assimilation of SMOS brightness temperatures in the ECMWF integrated forecasting system. *Quart. J. Roy. Meteor. Soc.*, **145**, 2524–2548, <https://doi.org/10.1002/qj.3577>.

Palecki, M. A., J. H. Lawrimore, R. D. Leeper, J. E. Bell, S. Embler, and N. Casey, 2013: United States Climate Reference Network Products, Daily. NOAA/National Centers for Environmental Information, accessed 11 November 2021, <https://doi.org/10.7289/V5H13007>.

Pan, M., X. Cai, N. W. Chaney, D. Entekhabi, and E. F. Wood, 2016: An initial assessment of SMAP soil moisture retrievals using high-resolution model simulations and in situ observations. *Geophys. Res. Lett.*, **43**, 9662–9668, <https://doi.org/10.1002/2016GL069964>.

Quiring, S. M., T. W. Ford, J. K. Wang, A. Khong, E. Harris, T. Lindgren, D. W. Goldberg, and Z. Li, 2016: The North American soil moisture database: Development and applications. *Bull. Amer. Meteor. Soc.*, **97**, 1441–1459, <https://doi.org/10.1175/BAMS-D-13-00263.1>.

Rigden, A. J., R. S. Powell, A. Trevino, K. A. McColl, and P. Huybers, 2020: Microwave retrievals of soil moisture improve grassland wildfire predictions. *Geophys. Res. Lett.*, **47**, e2020GL091410, <https://doi.org/10.1029/2020GL091410>.

Robock, A., K. Y. Vinnikov, C. A. Schlosser, N. A. Speranskaya, and Y. Xue, 1995: Use of midlatitude soil moisture and meteorological observations to validate soil moisture simulations with biosphere and bucket models. *J. Climate*, **8**, 15–35, [https://doi.org/10.1175/1520-0442\(1995\)008<0015:UOMSMA>2.0.CO;2](https://doi.org/10.1175/1520-0442(1995)008<0015:UOMSMA>2.0.CO;2).

—, and Coauthors, 2003: Evaluation of the North American Land Data Assimilation System over the southern Great Plains during the warm season. *J. Geophys. Res.*, **108**, 8846, <https://doi.org/10.1029/2002JD003245>.

SCAN, 2016: SCAN daily historic provisional data. USDA National Resources Conservation Service National Water and Climate Center, accessed 16 February 2022, www.wcc.nrcs.usda.gov/scan.

Schaefer, G. L., M. H. Cosh, and T. J. Jackson, 2007: The USDA natural resources conservation service Soil Climate Analysis Network (SCAN). *J. Atmos. Oceanic Technol.*, **24**, 2073–2077, <https://doi.org/10.1175/2007JTECHA930.1>.

Shellito, P. J., and Coauthors, 2016: SMAP soil moisture drying more rapid than observed in situ following rainfall events. *Geophys. Res. Lett.*, **43**, 8068–8075, <https://doi.org/10.1002/2016GL069946>.

Smirnova, T. G., J. M. Brown, and S. G. Benjamin, 1997: Performance of different soil model configurations in simulating ground surface temperature and surface fluxes. *Mon. Wea. Rev.*, **125**, 1870–1884, [https://doi.org/10.1175/1520-0493\(1997\)125<1870:PODSMC>2.0.CO;2](https://doi.org/10.1175/1520-0493(1997)125<1870:PODSMC>2.0.CO;2).

—, —, —, and D. Kim, 2000: Parameterization of cold-season processes in the MAPS land-surface scheme. *J. Geophys. Res.*, **105**, 4077–4086, <https://doi.org/10.1029/1999JD901047>.

—, —, —, and J. S. Kenyon, 2016: Modifications to the Rapid Update Cycle Land Surface Model (RUC LSM) available in the Weather Research and Forecasting (WRF) Model. *Mon. Wea. Rev.*, **144**, 1851–1865, <https://doi.org/10.1175/MWR-D-15-0198.1>.

Svoboda, M., and Coauthors, 2002: The drought monitor. *Bull. Amer. Meteor. Soc.*, **83**, 1181–1190, <https://doi.org/10.1175/1520-0477-83.8.1181>.

Taylor, C. M., A. Gounou, F. Guichard, P. P. Harris, R. J. Ellis, F. Couvreux, and M. De Kauwe, 2011: Frequency of Sahelian storm initiation enhanced over mesoscale soil-moisture patterns. *Nat. Geosci.*, **4**, 430–433, <https://doi.org/10.1038/ngeo1173>.

van den Dool, H., J. Huang, and Y. Fan, 2003: Performance and analysis of the constructed analogue method applied to U.S. soil moisture over 1981–2001. *J. Geophys. Res.*, **108**, 8617, <https://doi.org/10.1029/2002JD003114>.

Vinnikov, K. Y., and I. B. Yeserkepova, 1991: Soil moisture: Empirical data and model results. *J. Climate*, **4**, 66–79, [https://doi.org/10.1175/1520-0442\(1991\)004<0066:SMEDAM>2.0.CO;2](https://doi.org/10.1175/1520-0442(1991)004<0066:SMEDAM>2.0.CO;2).

Wan, T., B. H. Covert, C. N. Kroll, and C. R. Ferguson, 2022: An assessment of the national water model's ability to reproduce drought series in the northeastern United States. *J. Hydrometer*, **23**, 1929–1943, <https://doi.org/10.1175/JHM-D-21-0226.1>.

Xia, Y., and Coauthors, 2012: Continental-scale water and energy flux analysis and validation for the North American Land Data Assimilation System project phase 2 (NLDAS-2):

1. Intercomparison and application of model products. *J. Geophys. Res.*, **117**, D03109, <https://doi.org/10.1029/2011JD016048>.

—, J. Sheffield, M. B. Ek, J. Dong, N. Chaney, H. Wei, J. Meng, and E. F. Wood, 2014: Evaluation of multi-model simulated soil moisture in NLDAS-2. *J. Hydrol.*, **512**, 107–125, <https://doi.org/10.1016/j.jhydrol.2014.02.027>.

—, M. B. Ek, Y. Wu, T. Ford, and S. M. Quiring, 2015a: Comparison of NLDAS-2 simulated and NASMD observed daily soil moisture. Part I: Comparison and analysis. *J. Hydrometeorol.*, **16**, 1962–1980, <https://doi.org/10.1175/JHM-D-14-0096.1>.

—, —, —, —, and —, 2015b: Comparison of NLDAS-2 simulated and NASMD observed daily soil moisture. Part II: Impact of soil texture classification and vegetation type mismatches. *J. Hydrometeorol.*, **16**, 1981–2000, <https://doi.org/10.1175/JHM-D-14-0097.1>.

Yao, Y., P. Ciais, N. Viovy, W. Li, F. Cresto-Aleina, H. Yang, E. Joetzjer, and B. Bond-Lamberty, 2021: A data-driven global soil heterotrophic respiration dataset and the drivers of its inter-annual variability. *Global Biogeochem. Cycles*, **35**, e2020GB006918, <https://doi.org/10.1029/2020GB006918>.